

Learning to reason about and to act on physical cascading events

Yuval Atzmon^{*1} Eli A. Meirom^{*1} Shie Mannor¹² Gal Chechik¹³

Abstract

Reasoning and interacting with dynamic environments is a fundamental problem in AI, but it becomes extremely challenging when actions can trigger cascades of cross-dependant events. We introduce a new supervised learning setup called *Cascade* where an agent is shown a video of a physically simulated dynamic scene, and is asked to *intervene* and trigger a cascade of events, such that the system reaches a "counterfactual" goal. For instance, the agent may be asked to "Make the blue ball hit the red one, by pushing the green ball". The agent intervention is drawn from a continuous space, and cascades of events makes the dynamics highly non-linear.

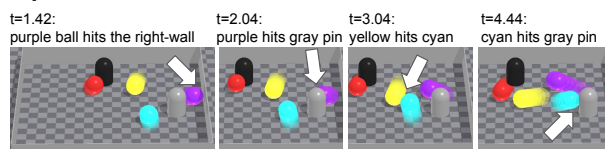
We combine semantic tree search with an event-driven forward model and devise an algorithm that learns to search in semantic trees in continuous spaces. We demonstrate that our approach learns to effectively follow instructions to intervene in previously unseen complex scenes. It can also reason about alternative outcomes, when provided an observed cascade of events.

1. Introduction

Cascades of events are wide-spread phenomena found in dynamical systems from biology (gene expression) and physics (meteorology) to chemistry and economics (supply chains). People can reason about such cascades and plan how to intervene to achieve a desired outcome of a system. This builds on several human capacities: inferring causal relations, reasoning in a counterfactual way about possible alternative dynamics of a system, and describing the goal in natural, semantic, language. Cascading dynamical systems are therefore a fantastic test bed for studying complex reasoning. But, how can we train computational agents to reason and intervene in a cascading dynamical system?

Here we address this question in a simulated dynamical system of a physical world, where object interactions form

Input 1: An observed cascade:



Input 2: An instruction:

"Push the purple ball to make the yellow hit the red, causing the yellow to hit the black pin within 4 collisions in the chain."

Output: A solution:



Figure 1. **The Cascade learning setup.** **Top:** A set of balls move freely in a confined space. Balls may collide with walls and static pins (grey & black cylinders) and yield an "observed" cascade of events. Arrows highlight each collision. **Middle:** A semantic instruction is given, partially describing an alternative ("counterfactual") cascade of events. **Bottom:** The agent is allowed to intervene and set the (continuous, 2D) initial velocity of the purple ball (the "pivot") to achieve the "counterfactual" cascade of events. Only showing key frames for brevity. See the videos side by side here: <https://youtu.be/u1Io-ZWC1Sw> (Anonymous)

a cascade of events. We describe a new supervised learning setup, called *Cascade* (Figure 1). In this setup, an agent observes a cascade of events in a system of moving and static objects. It is then provided with a desired goal for the system described in semantic terms. The agent may intervene and manipulate one object to achieve the goal.

More concretely, we consider the following supervised learning setup. At training time, the agent is given the initial conditions and object trajectories of an observed cascade, a semantic goal, and the initial conditions and trajectories of one possible solution. At test time, we sample a *new* unseen system and goal. The agent only has access to the goal and the "observed" cascade, and it should predict how to change the initial conditions to meet the goal.

This problem is very challenging and for several reasons. First, the intervention space is continuous, but is fragmented into many regions, each yielding a different outcome. The boundaries of these regions are hard and with no clear sub-

^{*}Equal contribution ¹NVIDIA Research, Israel ²Technion, Israel institute of technology ³Bar Ilan University, Israel. Correspondence to: Yuval Atzmon <yatzmon@nvidia.com>.

modularity, since a slight change in movement direction can yield a qualitatively different final outcome. This “butterfly effect” is indeed common in many cascading systems. As a result, it is hard to apply standard planning algorithms or gradient-based methods.

To further illustrate the difficulty of this task, consider how hard it is to even apply a “brute-force” approach. Such an approach would actually require access to a simulator of the system to test millions of candidate interventions. Then, one would also need to train a discriminator to decide if the simulation output satisfies the instruction goal, which is hard by itself. Needless to say, searching exhaustively over the space of possible interventions is not feasible. Another approach would be to train a regression model that takes the semantic goal and a representation of the “observed” cascade and outputs the predicted intervention. Below, we describe our experiments with this approach and explain why such fully differentiable approaches struggle in our problem.

Here, we design a representation that focuses on the semantics of the system dynamics (Figure 2). We call it an *Event Tree*. Specifically, we only keep key events where objects interact. In our physical system, these semantic events are collisions of balls, pins, and walls. We use these collisions to build a tree of possible behaviors of the system. In this tree, each node corresponds to a possible collision event. Every node i is connected to its children i_1, \dots, i_k which correspond to k realizable future collisions. A path in the tree therefore captures a realizable sequence of collisions. This representation also implies a tessellation of the space of possible interventions. Each intervention (a point in the intervention space) dictates a path in the event tree. Similar interventions often follow the same path.

To build this event tree, we assume that we have access to a special kind of forward model operating at the level of semantic events. For any given initial condition, we can query the forward model for the next event (e.g., “which objects collide next?”), and predict the outcome of that event (the directions and velocities of objects after they collided). Importantly, every node in the event tree is assigned a value. We learn a function that assigns values to nodes conditioned on the instruction.

At inference time, the event tree allows us to search efficiently over the space of interventions. Since the forward model is extremely lightweight, we can compute the fate of millions of possible interventions in parallel on a GPU. To find the best path, we first sample points in the intervention space, then iteratively compute the event path of each intervention. Finally, we select the node with the highest value.

Finally, we propose a simple approach for “counterfactual”

reasoning that uses the observed cascade. We first find the path in the event tree that corresponds to the observed video. Then, we perform a tree search in the event tree and explore first those paths that split off that observed path.

This paper makes the following contributions: (1) A new learning setup, *Cascade*, where an agent observes a dynamical system and then changes its initial conditions to meet a given semantic goal. (2) A data structure – *Event Tree* – and a principled probabilistic value function for searching efficiently over the space of interventions. (3) A method to transform a tree path into a Directed Acyclic Graph and learn its value function using a Graph Neural Network. (4) A method to use observed cascades to guide the search in the event tree towards a “counterfactual” outcome of the system.

2. Related work

Learning and reasoning in physical systems: Fragkiadaki et al. (2016); Battaglia et al. (2016); Lerer et al. (2016); Watters et al. (2017); Janner et al. (2019), learn physical forward models that focus on object interactions. Learning a forward model is out of the scope of this paper. Additionally, the former works use a fixed time step, rather than an adaptive time step like we do and like (Janner et al., 2019) that predicted the effects of an action in a single step.

CLEVRER, CRAFT, CATER and IntPhys (Yi et al., 2020; Ates et al., 2021; Girdhar & Ramanan, 2020; Riochet et al., 2018) are video understanding benchmarks, exploring reasoning over observed temporal and causal structures. CoPhy Baradel et al. (2020) studied counterfactual learning of object mechanics from visual input. These works differ than ours in a few key aspects. (1) They focus on understanding, question answering and tracking rather than taking an action as *Cascade* do. (2) The approaches in CLEVRER and CoPhy are based on a forward model with a fixed time-step. (3) CoPhy uses the observed video to estimate the value of a *static* property like gravity, while our setup reasons about the dynamic evolution of the observed cascade.

Roussel et al. (2019) studied the chain reaction problem, but their focus is different than ours. Their cascading configuration is known and they study how to robustly tune that configuration using a simulator. Our work focuses on *finding* a cascading configuration given a partial semantic description of it.

Planning: There is a large body of literature on following instructions in vision, action, and robotics (Reckman et al., 2010; Tellex et al., 2011; Chen & Mooney, 2011; Duvallet et al., 2013; Hemachandra et al., 2015; Andreas & Klein, 2015; Misra et al., 2017; Janner et al., 2018; Anderson et al., 2018; Krantz et al., 2020; Qi et al., 2020; Blukis et al., 2019; 2020; Luketina et al., 2019; Ichter et al., 2021; Driess et al.,

2020; Simeonov et al., 2020; Shridhar et al., 2021; Paxton et al., 2021; Schmeckpeper et al., 2020; Zhu et al., 2017). However, the problem we try to solve is inherently not a standard planning problem. An action is taken essentially only once and there is no way to change the ensuing cascade of events using additional actions ("Fire and forget"). This problem is a complex search problem which one can conceivably try to solve as such using brute-force methods or using some metaheuristic approaches.

3. Cascade: A benchmark for reasoning and intervening in a cascading dynamics.

We designed a new environment for evaluating reasoning and intervening in cascading events. The environment combines visual and physical modalities with semantics and action (Figure 1).

Scenes. Each scene describes a unique dynamical system. In these systems, several spheres move freely on a frictionless table, colliding with each other and with static pins within a confined four-walled space (Figure 1). Each episode describes a different scene, which includes tens of collisions. The agent is provided with (1) An "observed" (unperturbed) video of the evolution of this system; and (2) The initial position and velocity of each object.

Instructions. An instruction describes (1) A set of target semantic events (collisions) to be fulfilled "*Make the red ball hit the black pin*"; (2) A pivot object to manipulate "*You can push the green*"; and (3) constraints, of two possible types, that encourage the agent to reason about the cascade of events. The first type is a "count" constraint. It resembles constraining the total amount of resources available on a logistic chain. By determining an accumulated number of collisions, on *all* the paths from the pivot to the target collision, e.g. "*Within 3 collisions in the chain*". The second type is an "ancestor" constraint. It resembles having a bottleneck along on a logistic chain. By enforcing a specific collision that lies on *any* path that starts from the pivot and causes the target collision, e.g. "*It should include hitting the top wall with the red*". Section D.2 describes the instruction generation process. Section A provides more examples.

This paper focuses on the reasoning task. We therefore assume perfect visual and lexical perception and provide the agent with the ground-truth trajectories of objects, with collision labels, and with a structured vector representation of the instruction.

The agent's goal. The objective of the agent is to intervene with the initial conditions of the scene, by setting the velocity vector of the pivot object to reach a set of collisions specified by the instruction. This often requires a highly precise "trick shot", that takes into account detailed reasoning on how downstream events will roll out. Our instruction

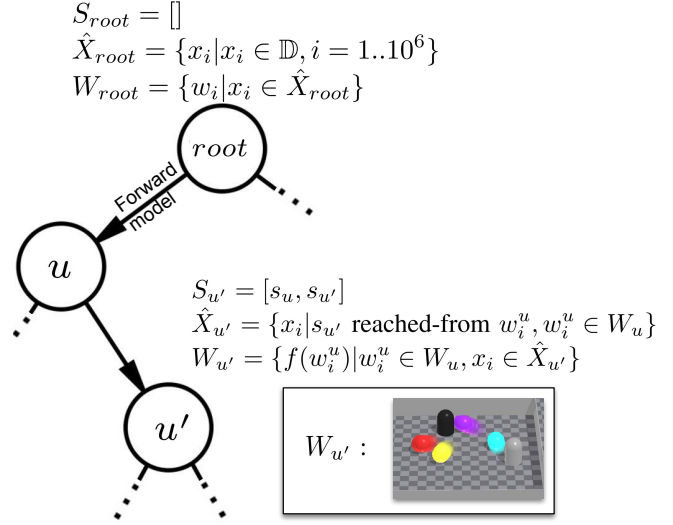


Figure 2. Illustration of the event tree data structure.

generation process guarantees that a solution exists for a given instruction. Namely, there are feasible intervention values that generate a sequence of events that satisfy the instruction.

The problem setup. An agent is given three inputs: An initial condition of the system, an "observed" cascade (e.g., a video) of the system that starts from these initial conditions, and a semantic instruction. The agent is asked to intervene by controlling one "pivot object" in the scene. It is allowed to adjust its velocity (movement direction and speed) to any value in a bounded set of possible interventions $\mathcal{X} \subset \mathbb{R}^d$. Given an instruction g , there exists a subset of possible solutions of \mathcal{X} that, when played out in the real-world, will satisfy the goal g . The goal is to predict an intervention $x \in \mathcal{X}$ that fulfills the instruction g .

During training, the following information is available: (1) A vector representation of the instruction g ; (2) An "observed" cascade of events of the system, assuming perfect perception - including the system initial conditions, the trajectories of the objects and a respective sequence of collisions; and (3) A "counterfactual" cascade of events of the system, which is one possible rollout of the system that fulfills the instruction. It includes a successful intervention in the initial conditions of the pivot, the object trajectories, and their collision sequence.

At inference time, the agent is only given the instruction and the "observed" cascade, and it should predict how to correctly intervene on the pivot initial conditions.

4. Methods

Before describing our approach, let us first motivate the reasons for using a forward model and tree search in our supervised learning setup, by describing the difficulties in

learning a more standard neural architecture.

Consider a fully differentiable model that takes the instruction and initial configuration and outputs a predicted intervention. Unfortunately, because the dynamics and goal of a problem are defined through discrete semantic events ("A hits B") in our continuous intervention space, there are "boundaries", such that a small deviation that crosses the boundary yields a qualitatively different final outcome. This fragments the continuous intervention space into many discrete regions in a way that depends on the semantic instruction. As a result, and since the goal is described in semantic terms, the problem must take into account the non-continuous nature of the dynamics and the symbolic-like nature of the goal. In problems that involve discrete and symbolic reasoning, neural approaches often struggle unless provided with proper inductive bias. Our approach uses our knowledge of the cascade problem structure in designing the solution.

Our proposed approach focuses on key "semantic" events of the dynamics (e.g., collisions). We build a tree of possible outcomes such that a path in the tree captures a realizable cascade of events. In addition, we learn a function that assigns values to tree nodes conditioned on the instruction. In inference time, we use the predicted node values to search efficiently over the space of interventions.

Next, we describe each component in more detail. First, we explain how to construct the semantic tree. Then, we elaborate on learning a value function over tree nodes, conditioned on a goal. Last, we describe the inference procedure.

4.1. The tree of possible futures

We now describe the main data structure that we use to represent the search problem - the *Event Tree*.

The event tree is designed to provide a searchable data structure for sequences of events that are physically realizable. To make these searches efficient, we represent the system behavior at the *semantic* level. In our concrete physical example, a semantic event s_i is a collision between two object (for example, the yellow ball "hits" the right wall). In other systems, these could be any key interactions between system components, like "opening" a lid in video reasoning, "manufacturing" an item in supply chains, a protein "binding" the DNA to regulate the expression of a gene. Importantly, in our approach, we require that it is possible to compute the state of the system right after an event.

In our event tree, each node corresponds to a sequence of semantic events. The children of each node correspond to realizable continuations of the event sequence. Namely, all possible events that could happen after the sequence S_u . We now formally describe the properties of nodes and how we build the edges of the Event Tree.

Tree Nodes. A node u of the event tree represents a sequence of semantic events $S_u \triangleq (s_1, s_2, \dots, s_u)$.

Note that there could be many interventions in \mathcal{X} that lead to the same sequence of events S_u . As a result, a node also corresponds to the subset of interventions $X_u \subset \mathcal{X}$ that yields the sequence of events S_u . More formally, we aggregate to a common node all interventions $x \in \mathcal{X}$ that result in the same sequence prefix. In practice, instead of keeping a representation of the full subset X_u , we sample the space of interventions, and collect, say, 10^6 points $\hat{X}_0 = \{x_i | x_i \in \mathcal{X}, i = 1 \dots 10^6\}$. All samples that yield a sequence S_u therefore form an estimate of X_u : $\hat{X}_u = \{x_i | x_i \in \mathcal{X}, i = 1..10^6, x_i \text{ yields } S_u\}$.

The root node describes the dynamical system at $t = 0$ and its sequence of events S_{root} is empty. Its *intervention subset* is $X_{root} = \mathcal{X}$. All sampled interventions are mapped to the root node $\hat{X}_{root} = \hat{X}_0$. See Figure 2, top.

For every node, we also keep the *world-state* W_u , which is the set of physical configurations of the system after yielding the sequence S_u , for every $x \in \hat{X}_u$. A sample world state w_i^u is the world state for the sampled intervention x_i after following the sequence until S_u . See Figure 2. In our physical setup, the dynamics are prescribed by the position and velocity $c_i^j = (pos_i^j, vel_i^j), j = 1 \dots n$ of each of n objects in the environment (we omitted u for brevity). The world state w_i^u is then a tuple $w_i^u = (c_i^1, c_i^2, \dots, c_i^n, t_i)$, where for the root node $t_i = 0$ for all x_i . Correspondingly, the *world state set* of a node u is $W_u = \{w_i | x_i \in X_u\}$.

Given the world state of a current node, we then ask for the next immediate event (next feasible immediate collision).

An event-driven forward model. The goal of the forward model is to uncover which semantic events may occur next. Conceptually, our model takes as input a world-state w_i and outputs the next immediate semantic event. Our forward model $f(\cdot)$ is not a full fledged simulator as it does not propagate time at discrete time steps but solves a set of analytic equations to find the event time, should one occur. Formally, given an input world state w_i it outputs the next semantic event (s'), and dynamic configuration $f(w_i) = w_i' = (c_i'^1, c_i'^2, \dots, c_i'^n, t_i')$ immediately after the predicted semantic event at t_i' .

Our lightweight model is easily parallelizable and allows us to quickly detect possible futures for multiple world states simultaneously, as detailed in the appendix. However, our model only provides an *approximation* of the dynamics of our test bed environment, and its predictions differ from detailed physical simulators such as IsaacGym (Makoviychuk et al., 2021) and PyBullet (Coumans & Bai, 2016). This difference is because simulators operate with fixed, small timesteps whereas we our lightweight model makes large, adaptive steps, and also due to numerical issues and

various relaxations. As discussed above, small deviations in the initial configuration yield qualitative changes. Hence, the dynamics predicted by our forward model differ than those of the simulators, and these differences exacerbate along the cascade. These sim-to-sim differences mimic the sim-to-real problem. Importantly, by using an event-driven model we reduce the errors accumulated during simulation.

Node Expansion. Suppose we decide to expand a node u . We apply the forward model $f(\cdot)$ to each world state $w_i \in W^u$. We then aggregate all the propagated world states which share the same immediate next semantic event s' to a new node u' : The event sequence of the child node u' is $S_{u'} = \text{concat}(S_u, s')$, the corresponding interventions are $X_{u'} = \{x_i | s' \text{ reached-from } w_i\}$ and $W_{u'} = \{f(w_i) | w_i \in W_u, x_i \in X_{u'}\}$. Note that we replaced $(x_i \text{ yields } S_{u'})$ with $(s' \text{ reached-from } w_i)$, because they are equivalent when expanding recursively the former.

Expanding the tree can be viewed as a tessellation refinement of the intervention space \mathcal{X} . At each step, we pick one cell and split it into multiple cells, where each child cell represents a different event that occurs after a shared sequence of events, represented by the parent cell.

If the tree is fully expanded, it covers all possible futures. However, expanding the whole tree is expansive, because the branching ratio, or the number of events, grows quadratically with the number of objects. In the next subsection, we discuss how we learn a scoring function and use it to guide an efficient tree search.

4.2. Learning the value function

To find a node that satisfies the goal, we prioritize which node to expand by learning a value function that is conditioned on the instruction g , in a supervised manner.

We propose to take a principled probabilistic approach for setting the value function. Setting it to the likelihood that the sequence of events of $x \in X_u$ will satisfy the goal g ,

$$V(u) = \Pr(x \text{ satisfies } g | g, x \in X_u), \quad (1)$$

This probabilistic perspective allows us to take a maximum-likelihood approach at inference time and prioritize nodes according to a maximum-likelihood policy.

In practice, to calculate the value labels for training, we use the maximum likelihood estimate of Eq. (1). Namely, for every node u along the counterfactual sequence, we take the fraction of the sample set that reaches the node (u_g) that satisfies the instruction.

$$\hat{\Pr}(x_i \in X_{u_g} | g, x_i \in X_u) = \|X_{u_g}\| / \|X_u\|. \quad (2)$$

For every node outside that sequence, we set its value to 0.

In the experimental Section 5 we also explore alternative approaches for assigning ground-truth values to nodes.

A model for the value function. Next, we describe the representation and architecture for modelling a node value function. The model takes as inputs the instruction g and sequence of events S_u that define the node u , and predicts a scalar value with ground-truth labels according to Eq. (2).

Since S_u is a sequence of events, it would be natural to use a sequential representation that is conditioned on the instruction. However, although this representation is temporarily ordered, it does not convey well the relations describing the cascade of events. E.g. In the following sequence of collisions $[(A, B), (C, D), (A, E)]$, the collision (A,E) is affected by (A,B), because A is common for both, while (C,D) is less relevant for describing the events that lead to (A,E).

Therefore, we propose to transform each sequence to a Directed Acyclic Graph (DAG) that captures relations in the cascade of events. A node in this DAG is an event that involves some objects (a collision), and each edge represents a dynamic (moving) object shared by two subsequent events. See Figure 3 for a concrete illustration.

We note that this representation is useful for reasoning about semantic instructions, but we intentionally refrain from naming it a *Causal* DAG, because it does not respects the formal Causal-Inference definition of a causal model (Pearl, 2000). More discussion in appendix (Section B).

Architecture We use a Graph Neural Network (GNN) to parameterize our value function. We represent the graph as a tuple (A, X, E, z) where $A \in \{0, 1\}^{n \times n}$ is the graph adjacency matrix, $X \in \mathbb{R}^{n \times d}$ is a node feature matrix, $E \in \mathbb{R}^{m \times d'}$ is an edge feature matrix, and $z \in \mathbb{R}^{d''}$ is a global graph feature. We chose to use a popular message passing GNN model (Battaglia et al., 2018) that maintains learnable node, edge and global graph representations. We describe the model architecture and feature matrices in detail in the appendix (Section E).

4.3. Inference

Our agent searches the tree for the maximum valued node u_{MAX} . Then, it randomly selects an intervention from its intervention subset $x \in X_{u_{MAX}}$. We consider two variants.

Interventional search: The agent performs a tree search for the highest valued node. At any given step, the agent stores a sorted list of nodes together with their values, it then picks the highest valued node from this list and expands it. The node children are then added to the list with their predicted values, and the agent resorts the list.

We limit the tree search to expand only 80 nodes, whereas a full event tree, which contains all possible realizations, have billions of nodes, $\sim \times 2.8$ per unit of depth (empirically).

Counterfactual search: To improve the interventional search, we propose a simple approach to use the *observed*

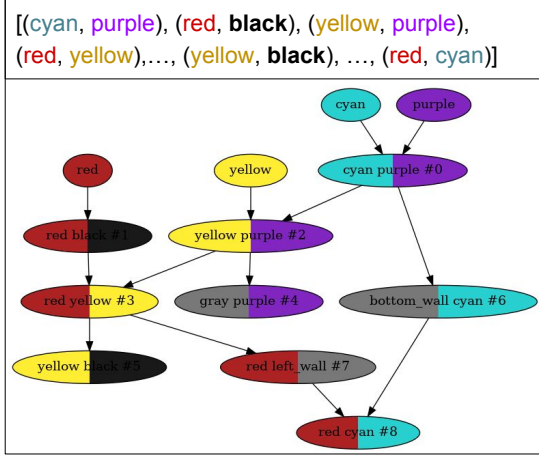


Figure 3. Illustrating how a sequence of events (top) is transformed to a DAG (bottom). It corresponds to the video in Figure 1 bottom.

cascade during inference. Consider the case where the sequence of the solution is complex (long sequence) and the *observed* sequence diverges from the solution at a late point. In this case, it is likely that the observed will be informative about the solution. To use that information when exploring the search space, we start the search by expanding the nodes along the observed sequence: For each observed node, we add its children to the sorted list described above together with their predicted values. After that point, we continue the search as described by the “Interventional search”.

In practice, we only expand $N_{observed}$ nodes from every observed sequence, where $N_{observed}$ is a hyper-parameter.

5. Experiments

Next, we describe our experimental protocol, compared methods, and evaluation metrics.

5.1. Dataset

We generated a dataset following the procedure described in Section D. Specifically, we sampled $\sim 46K$ scenes, each includes 4-6 moving balls, 0-2 pins, and 4 walls and up to 5 semantic instructions (~ 4.25 on average). An episode is a pair of a scene and one instruction. Data is split by unique *scenes* rather than by episodes, keeping 470 unique, unseen scenes for test (~ 2000 episodes), 69 scenes for selecting hyper-parameters (val. set), and the rest are used for training.

For calculating the training labels of the value function, we traverse the semantic tree along the ground-truth sequence of the “counterfactual” cascade, and collect the positive labels using Eq. (2). If the event tree cannot reproduce the “counterfactual” sequence of a sample (due to errors accumulating by the forward model), then Eq. (2) cannot be calculated, and we drop that sample from the training set.

We collect negative samples (with $V = 0$) by (1) taking the child nodes that diverge from the path to the ground-truth. (2) Traverse a random path along the tree with the same length as the ground truth sequence, and set the value of all the nodes along that path to 0. In total, this offline stage yields $\sim 6.8M$ training samples for the value function.

5.2. Hyper parameters

We train the model and baselines for 15 epochs. Batch size was set to 8192 to maximize the GPU memory usage. We use the PyTorch’ default learning rate for Adam (Kingma & Ba, 2015) (0.001). For inference, we set $N_{observed}$ to 8, the maximal tree depth to 30, we sample 10^6 initial conditions and expand 80 nodes per episode which takes ~ 13 seconds. The GNN uses 5 layers, with a hidden state dimension of 128. Hyper parameters were tuned one at a time, during an early experiment on a validation set.

5.3. Compared Methods

ROSETTE (Reasoning On SEmanTic TreEs): This is our full-fledged approach. Searching in semantic trees, by learning a goal conditioned value function, with a DAG representation and a GNN architecture. Search uses the “counterfactual” variant of the tree search (Section 4.3), by first expanding the nodes along the “observed” sequence.

ROSETTE-IV: Like ROSETTE, but using “Interventional search” (Section 4.3) - not using the “observed” sequence. For a fair comparison, we make sure that ROSETTE expands the same number of nodes in total as ROSETTE-IV.

SEQUENTIAL: Using a sequential representation for a tree chain, instead of a DAG. Specifically, we represent the sequence as a graph with edges along the sequence. (Litany et al., 2022) compared a recursive versus standard synchronous propagation in GNN models and found them empirically equivalent.

Deep Sets regression: Embedding the instruction and the initial world state to predict a continuous intervention. We embed the objects’ initial positions and velocities using the permutation-invariant “Deep Sets” architecture (Zaheer et al., 2017), and use an L2 loss with respect to ground-truth interventions in the “counterfactual” training samples.

Random: Sample intervention at random from an estimated distribution of ground-truth interventions.

Brute force: We train a classifier for goal satisfaction, given a sequence of collisions, and exhaustively search using the event-driven forward model and 10^6 initial conditions. This baseline is equivalent to ROSETTE-IV, when using a Dirac Delta function as the value function.

We also carry a thorough ablation study: First, we compare the “Counterfactual search” to the “Interventional search” using a metric that focuses on episodes where the observed sequence may be beneficial. In addition, we emphasize

the effect of “Counterfactual search” by building a dataset with more complex instructions using a third constraint, and compare the two types of search across “Easy” and “Hard” instructions. We describe this dataset in Section D.4.

Second, we explore alternative approaches to assign ground-truth values to nodes along the ground-truth “counterfactual” sequence. **Linear**: Linearly increases the value by $V(u) = \text{depth}(u)/\text{depth}(u_g)$. **Step**: Give a fixed medium value to nodes along the sequence, and a maximal value to the target node: $V(u) = 0.5 + 0.5\mathbf{1}_{u_g}(u)$. **Dirac-Delta**: Sets $V(u) = \mathbf{1}_{u_g}(u)$, this baseline is equivalent to using a target node classifier as a value function.

Last, we test how ablating parts of the instruction affects the ROSETTE model performance. Implementation details of the baselines and ablations are described in Section C.

5.4. Evaluation metrics

For each episode and goal, we predict an intervention and evaluate their success rate using the following metrics.

Simulator success rate: The success rate when rolling out the predicted intervention using a physical simulator (Makoviychuk et al., 2021). This metric mimics experimenting in the real world.

Tree success rate (where applicable): We compare the sequence of semantic events from the selected node in our event tree with the events and constraints specified by the instruction. This metric allows us to evaluate the performance of the value function model and tree search, independently from the errors that may be introduced due to the event-driven forward model.

We further measured refinements of these metrics by conditioning on various properties of the instruction and scene.

(1) Condition tree success rate on instruction type: Unconstrained: The instruction only specifies target collisions. **Ancestor**: also contains an “ancestor” constraint. **Count**: contains a “count” constraint. **A&C**: contains both “ancestor” and “count” constraints.

(2) Condition tree success rate on instruction complexity: Instructions with 2 or more constraints are marked as “Hard”, and the rest as “Easy”. This metric was evaluated on the complex instruction dataset.

(3) Condition tree success rate on pivot first collision: that is, the starting point of the first collision of the pivot in the ground-truth “counterfactual” video. This metric allows us to evaluate how well the model leverages the information in the observed sequence. When “Pivot first collision” is small, many correct solutions may exist, other than the one in the dataset, and the observed sequence is less likely to be useful for the agent. However, if the pivot object comes into action in a late stage, it becomes more likely that the observed sequence will be useful. We aggregate the success rate over “Head” cases, where “Pivot 1st collision”

$\in \{1 \dots 5\}$, which covers $\sim 80\%$ of the test data, and the remaining “Tail” cases $\{6 \dots 19\}$.

For each metric, we report its mean value and standard error of the mean across 5 different model seeds.

	TREE	SIMULATOR
RANDOM	NA	$17.6 \pm 0.3\%$
DEEPMAP REGRESSION	NA	$18.4 \pm 0.5\%$
BRUTE FORCE	$33.5 \pm 1.6\%$	$33.5 \pm 1.2\%$
SEQUENTIAL	$52.3 \pm 0.8\%$	$43.3 \pm 0.2\%$
ROSETTE	$61.0 \pm 0.5\%$	$48.9 \pm 0.4\%$

Table 1. Success rate of our approach and baselines

	TREE
ROSETTE-IV (OURS)	$59.7 \pm 0.3\%$
LINEAR	$48.7 \pm 0.7\%$
STEP	$45.1 \pm 1.0\%$
DIRAC DELTA	$33.5 \pm 1.6\%$

Table 2. Tree success rate for variants of the value function.

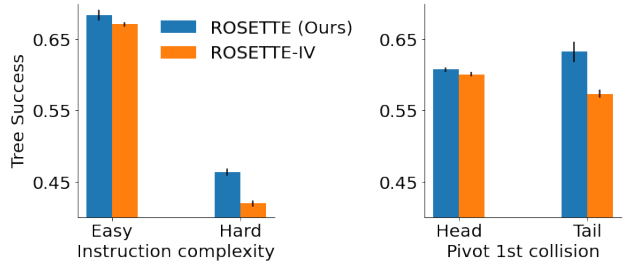


Figure 4. Comparing “Counterfactual search” (ROSETTE) with “Interventional” search (ROSETTE-IV) for 2 levels of instruction complexity (“Hard”: 2 or more constraints) and the starting point of the pivot in the sequence (“Tail”: first pivot collision is greater than 5). ROSETTE does make use of the observed cascade in tree search and performs significantly better, showing improvement of 10.7% and 13% respectively.

6. Results

We first describe the performance of ROSETTE on the test set and compare them with baseline methods. We then study in greater depth the properties of ROSETTE, through a series of ablation experiments. Finally, we provide qualitative examples.

Table 1 describes the *Tree* and the *Simulator* success rates of ROSETTE and compared methods. ROSETTE achieves the highest success rate for both the “Tree” success rate (61%) and the “Simulated” success rate (48.9%). Achieving $\sim 80\%$ conversion rate from *Tree* to *Simulated*. The random baseline success rate is (17.6%), which is close to the performance of the regression model. We conjecture that the regression model fails, because it can’t “imagine”

Learning to reason about and to act on physical cascading events

	UNCONSTRAINED	ANCESTOR	COUNT	A & C
ROSETTE	78.0 \pm 0.9%	68.1 \pm 0.7%	58.1 \pm 1.1%	50.8 \pm 0.9%
SEQUENTIAL	76.7 \pm 0.5%	68.4 \pm 1.1%	44.4 \pm 1.3%	37.1 \pm 1.5%
INSTRUCTION -COUNT	76.9 \pm 0.8%	68.6 \pm 0.9%	8.0 \pm 0.4%	15.7 \pm 0.6%
INSTRUCTION -ANCESTOR	76.5 \pm 0.8%	24.2 \pm 1.2%	58.3 \pm 0.7%	36.4 \pm 0.6%
INSTRUCTION -COUNT -ANCESTOR	77.2 \pm 0.8%	24.4 \pm 0.8%	8.1 \pm 0.5%	5.4 \pm 0.2%
INSTRUCTION -FULL	60.8 \pm 0.5%	32.7 \pm 0.9%	11.7 \pm 0.5%	6.6 \pm 0.1%

Table 3. Ablation study across 4 types of instructions. In red we denote results that perform significantly worse than ROSETTE.

the outcomes of the input configuration as ROSETTE can. When evaluating the brute force approach with same computational budget as ROSETTE, expanding 80 events, it performs largely worse than ROSETTE (33.5%). However, when allowing a $\times 20$ computational budget, expanding 4000 nodes (4.5 min/episode vs 13 sec/episode), it reaches a similar success rate as ROSETTE ($Tree = 61.9\%$, $Simulated = 53.8\%$). The Sequential approach is the strongest baseline, reaching $Tree = 52.3\%$ and $Simulated = 43.4\%$ success rates. We study the strengths and weaknesses of this baseline in the ablation experiments. Last, we notice that the weaker baselines have better conversion rate from $Tree$ to $Simulated$, this is likely because the weaker baselines find solutions for easier goals, with a short chain from the pivot to the target, and therefore accumulate less errors of the forward model along the way.

6.1. Ablation experiments

To understand the contribution of the different components of ROSETTE, we carried out a set of ablation experiments that quantify the benefits of (1) Using the “Counterfactual search” (Fig 4) (2) Various value functions, (Table 2) and (3) The effect of instruction complexity (Table 3).

Figure 4 quantifies the benefit gained by using “Counterfactual” (ROSETTE) over “Interventional” (ROSETTE-IV) search (Section 4.3). ROSETTE shows a relative improvement 10.7% (46.4% vs 41.9%) for complex instructions, and 13% for late start cascades (64.1% vs 56.7%).

Table 2 shows the advantage of the probabilistic formulation of the value function (ROSETTE-IV), compared to the several heuristics described in Section 5: The strongest baseline (“Linear”) only reaches 48.7% vs. 59.7% for ROSETTE-IV.

Table 3 allows an in-depth examination of the strengths and weaknesses of ROSETTE, dissecting the success rate across 4 types of instructions, as described in Section 5. We compare ROSETTE with its sequential alternative, and examine how ablating parts of the instruction affects the ROSETTE model performance. First, we observe that the sequential baseline can find target collisions that depend on an ancestor collision, as well as ROSETTE. However, it fails with “count” instructions (37.1% vs 50.8%), since it has no capacity for that reasoning task. Second, we observe that

ROSETTE effectively uses the instruction, since any part of the instruction that gets ablated only hurts its respective success rate.

6.2. Qualitative Examples

Here we provide links to qualitative examples we uploaded to YouTube, best viewed in $\times 0.25$ slow motion. The YouTube account we use is anonymous. In Section A, we explain every example in detail and provide more examples.

We compare ROSETTE successes with ROSETTE-IV failures. For each episode, we show a side-to-side video of the observed cascade, the ROSETTE successful case, and ROSETTE-IV failure case. The instruction is displayed on top of each video. [link #1](#), [link #2](#), [link #3](#), [link #4](#), [link #5](#), [link #6](#). Importantly, the examples demonstrate the usefulness of the observed cascade for tree search. ROSETTE followed the observed cascade along the part of the path that was useful to satisfy the instruction. It diverged from the path when necessary, and found a solution when long cascades were essential, while ROSETTE-IV struggled.

7. Discussion

We presented a new supervised learning setup, called *Cascade*, where an agent observes a cascade of events in a dynamical system and is asked to intervene and changes its initial conditions to meet a given semantic goal. We use an event tree representation and a principled probabilistic value function for searching efficiently over the space of interventions. In addition, we show that “hot starting” the tree search using the observed cascade of events improves the success rate.

Given an estimator for the value function learned by our approach, our tree search policy is greedy and rule-based. It remains an interesting question to use a learning-based policy that makes use of the observed cascade when searching the tree.

In this paper, we took a first step towards understanding how to affect a complex system of cascading events. In essence, we aim to learn how to use the butterfly effect in a positive manner. That is, how to modify the initial conditions of a complex system so that the desired outcomes are achieved.

References

- Anderson, P., Wu, Q., Teney, D., Bruce, J., Johnson, M., Sünderhauf, N., Reid, I., Gould, S., and Hengel, A. V. D. Vision-and-language navigation: Interpreting visually-grounded navigation instructions in real environments. *2018 IEEE/CVF Conference on Computer Vision and Pattern Recognition*, pp. 3674–3683, 2018.
- Andreas, J. and Klein, D. Alignment-based compositional semantics for instruction following. In *EMNLP*, 2015.
- Ates, T., Atesoglu, M. S., Yigit, C., Kesen, I., Kobas, M., Erdem, E., Erdem, A., Goksun, T., and Yuret, D. Craft: A benchmark for causal reasoning about forces and interactions, 2021.
- Baradel, F., Neverova, N., Mille, J., Mori, G., and Wolf, C. Cophy: Counterfactual learning of physical dynamics, 2020.
- Battaglia, P. W., Pascanu, R., Lai, M., Rezende, D., and Kavukcuoglu, K. Interaction networks for learning about objects, relations and physics. In *Advances in Neural Information Processing Systems (NeurIPS)*, 2016.
- Battaglia, P. W., Hamrick, J. B., Bapst, V., Sanchez-Gonzalez, A., Zambaldi, V., Malinowski, M., Tacchetti, A., Raposo, D., Santoro, A., Faulkner, R., Gulcehre, C., Song, F., Ballard, A., Gilmer, J., Dahl, G., Vaswani, A., Allen, K., Nash, C., Langston, V., Dyer, C., Heess, N., Wierstra, D., Kohli, P., Botvinick, M., Vinyals, O., Li, Y., and Pascanu, R. Relational inductive biases, deep learning, and graph networks, 2018.
- Blukis, V., Terme, Y., Niklasson, E., Knepper, R. A., and Artzi, Y. Learning to map natural language instructions to physical quadcopter control using simulated flight. In *CoRL*, 2019.
- Blukis, V., Knepper, R. A., and Artzi, Y. Few-shot object grounding and mapping for natural language robot instruction following. *ArXiv*, abs/2011.07384, 2020.
- Chen, D. L. and Mooney, R. Learning to interpret natural language navigation instructions from observations. In *AAAI 2011*, 2011.
- Coumans, E. and Bai, Y. Pybullet, a python module for physics simulation for games, robotics and machine learning, 2016.
- Driess, D., Ha, J.-S., and Toussaint, M. Deep visual reasoning: Learning to predict action sequences for task and motion planning from an initial scene image. In *Robotics: Science and System XVI*, Corvallis, OR, 2020. RSS Foundation. doi: 10.15607/RSS.2020.XVI.003. URL <http://www.roboticsproceedings.org/rss16/p003.html>; <http://www.roboticsproceedings.org/rss16/index.html>; <http://www.roboticsproceedings.org/>.
- Duvallet, F., Kollar, T., and Stentz, A. Imitation learning for natural language direction following through unknown environments. *2013 IEEE International Conference on Robotics and Automation*, pp. 1047–1053, 2013.
- Fragkiadaki, K., Agrawal, P., Levine, S., and Malik, J. Learning visual predictive models of physics for playing billiards, 2016.
- Girdhar, R. and Ramanan, D. Cater: A diagnostic dataset for compositional actions and temporal reasoning, 2020.
- Hagberg, A., Swart, P., and S Chult, D. Exploring network structure, dynamics, and function using networkx. Technical report, Los Alamos National Lab.(LANL), Los Alamos, NM (United States), 2008.
- Hemachandra, S., Duvallet, F., Howard, T. M., Roy, N., Stentz, A., and Walter, M. R. Learning models for following natural language directions in unknown environments. *2015 IEEE International Conference on Robotics and Automation (ICRA)*, pp. 5608–5615, 2015.
- Ichter, B., Sermanet, P., and Lynch, C. Broadly-exploring, local-policy trees for long-horizon task planning, 2021.
- Jänner, M., Narasimhan, K., and Barzilay, R. Representation learning for grounded spatial reasoning. *Transactions of the Association for Computational Linguistics*, 6:49–61, 2018.
- Janner, M., Levine, S., Freeman, W. T., Tenenbaum, J. B., Finn, C., and Wu, J. Reasoning about physical interactions with object-oriented prediction and planning. In *Proceedings of the International Conference on Learning Representations (ICLR)*, 2019.
- Kingma, D. and Ba, J. Adam: A method for stochastic optimization. In *ICLR*, 2015.
- Krantz, J., Wijmans, E., Majumdar, A., Batra, D., and Lee, S. Beyond the nav-graph: Vision-and-language navigation in continuous environments. *ArXiv*, abs/2004.02857, 2020.
- Lerer, A., Gross, S., and Fergus, R. Learning physical intuition of block towers by example, 2016.
- Litany, O., Maron, H., Acuna, D., Kautz, J., Chechik, G., and Fidler, S. Federated learning with heterogeneous architectures using graph hypernetworks, 2022.

- Luketina, J., Nardelli, N., Farquhar, G., Foerster, J. N., Andreas, J., Grefenstette, E., Whiteson, S., and Rocktäschel, T. A survey of reinforcement learning informed by natural language. In *IJCAI*, 2019.
- Makoviychuk, V., Wawrzyniak, L., Guo, Y., Lu, M., Storey, K., Macklin, M., Hoeller, D., Rudin, N., Allshire, A., Handa, A., and State, G. Isaac gym: High performance gpu-based physics simulation for robot learning, 2021.
- Misra, D. K., Langford, J., and Artzi, Y. Mapping instructions and visual observations to actions with reinforcement learning. In *EMNLP*, 2017.
- Paxton, C., Xie, C., Hermans, T., and Fox, D. Predicting stable configurations for semantic placement of novel objects, 2021.
- Pearl, J. *Causality: models, reasoning and inference*, volume 29. Springer, 2000.
- Qi, Y., Wu, Q., Anderson, P., Wang, X., Wang, W., Shen, C., and Hengel, A. V. D. Reverie: Remote embodied visual referring expression in real indoor environments. *2020 IEEE/CVF Conference on Computer Vision and Pattern Recognition (CVPR)*, pp. 9979–9988, 2020.
- Reckman, H., Orkin, J., and Roy, D. Learning meanings of words and constructions, grounded in a virtual game. In *KONVENS*, 2010.
- Riochet, R., Castro, M. Y., Bernard, M., Lerer, A., Fergus, R., Izard, V., and Dupoux, E. Intphys: A framework and benchmark for visual intuitive physics reasoning. *ArXiv*, 2018.
- Roussel, R., Cani, M.-P., Léon, J.-C., and Mitra, N. J. Designing chain reaction contraptions from causal graphs. *ACM Trans. Graph.*, 38(4), 2019. ISSN 0730-0301. doi: 10.1145/3306346.3322977. URL <https://doi.org/10.1145/3306346.3322977>.
- Schmeckpeper, K., Xie, A., Rybkin, O., Tian, S., Daniilidis, K., Levine, S., and Finn, C. Learning predictive models from observation and interaction, 2020.
- Shridhar, M., Manuelli, L., and Fox, D. Cliport: What and where pathways for robotic manipulation, 2021.
- Simeonov, A., Du, Y., Kim, B., Hogan, F. R., Tenenbaum, J., Agrawal, P., and Rodriguez, A. A long horizon planning framework for manipulating rigid pointcloud objects, 2020.
- Tellex, S., Kollar, T., Dickerson, S., Walter, M. R., Banerjee, A., Teller, S., and Roy, N. Approaching the symbol grounding problem with probabilistic graphical models. *AI Mag.*, 32:64–76, 2011.
- Watters, N., Tacchetti, A., Weber, T., Pascanu, R., Battaglia, P., and Zoran, D. Visual interaction networks. In *Advances in Neural Information Processing Systems (NeurIPS)*, 2017.
- Yi, K., Gan, C., Li, Y., Kohli, P., Wu, J., Torralba, A., and Tenenbaum, J. B. Clevrer: Collision events for video representation and reasoning, 2020.
- Zaheer, M., Kottur, S., Ravanbakhsh, S., Póczos, B., Salakhutdinov, R., and Smola, A. Deep sets. In *NIPS*, 2017.
- Zhu, Y., Gordon, D., Kolve, E., Fox, D., Fei-Fei, L., Gupta, A. K., Mottaghi, R., and Farhadi, A. Visual semantic planning using deep successor representations. *2017 IEEE International Conference on Computer Vision (ICCV)*, pp. 483–492, 2017.

Supplementary Information

A. Qualitative examples

Here we describe qualitative examples, and link to the corresponding videos on youtube. The videos are best viewed in $\times 0.25$ slow motion.

Comparing ROSETTE successes with ROSETTE-IV failures: Here we show winning cases of our approach (ROSETTE) doing “Counterfactual search” with respective failures of ROSETTE-IV that use a vanilla “Interventional search”. For each episode, we show a side-to-side video of the observed cascade, the ROSETTE successful case, and ROSETTE-IV failure case.

- *Push the green ball to make the yellow hit the blue, causing the green to strike the yellow within 5 collisions in the chain*

In this example, ROSETTE semantically follows the first 6 collisions as in the observed cascade. The green pivot comes into play on the 5th collision, and the agent adjusts its velocity such that it shall yield the goal. See the complete video here: <https://youtu.be/24rTpghzBeQ>

- *Push the cyan ball to make the cyan hit the black pin, causing the green to strike the gray pin within 5 collisions in the chain*

In this example, ROSETTE semantically follows the first 6 collisions as in the observed cascade, although the cyan pivot comes into play already on the 1st collision. The agent adjusts the pivot velocity such that it shall yield the goal. The ROSETTE-IV baseline completely fails. See the complete video here: <https://youtu.be/TZbUDNM6Qgs>

- *Push the cyan ball to make the cyan hit the bottom wall, causing the cyan to strike the red within 7 collisions in the chain*

In this example, ROSETTE semantically follows the first 9 collisions as in the observed cascade, although the cyan pivot comes into play already on the 2nd collision. The ROSETTE-IV baseline strikes the target collision, but fails with both the “ancestor” and “count” constraints. See the complete video here: <https://youtu.be/y3AVVMonG4s>

- *Push the yellow ball to make the yellow hit the cyan, causing the cyan to strike the black pin within 3 collisions in the chain*

In this example, ROSETTE semantically follows the first 5 collisions as in the observed cascade. The yellow pivot comes into play on the 4th collision.

The ROSETTE-IV baseline strikes the “ancestor” constraint, but fails to find the target collision. See the complete video here: <https://youtu.be/6DAGzlu8pfw>

- *Push the cyan ball to make the cyan strike the green within 4 collisions in the chain*

In this example, ROSETTE semantically follows the first 6 collisions as in the observed cascade. The cyan pivot comes into play on the 6th collision. The ROSETTE-IV baseline strikes the target collision, but fails on the “count” constraint. See the complete video here: <https://youtu.be/Jlq0-sSMoJk>

- *Push the cyan ball to make the cyan strike the gray pin within 6 collisions in the chain*

In this example, ROSETTE semantically follows the first 6 collisions as in the observed cascade, although the cyan pivot comes into play already on the 2nd collision. The agent adjusts the pivot velocity such that it shall yield the goal. The ROSETTE-IV baseline completely fails. See the complete video here: <https://youtu.be/C3b200U5n2I>

Successful episodes with ROSETTE-IV . Which is our approach, but using a vanilla “Interventional search”.

- In this example, the agent plans the trajectory of the blue ball, to wait for the red ball to bounce back from the left wall. Then the blue hits the red and sends it toward the black pin. See the complete video here: <https://youtu.be/AlMV1AyTR38>

- In the following example, the agent fulfills the “ancestor” constraint, making the cyan hit the top wall before it bounces back and makes the green to strike the blue. https://youtu.be/Y_XVFZ4RKY0.

- In the following example, the trajectory of the cyan ball is set away from any colliding balls. This makes the blue to passively strike the red. See the complete video here: <https://youtu.be/7QY34UxYaA8>

- In the following example, the agent fulfills both the “ancestor” constraint and the “count” constraint. <https://youtu.be/7otEWNs1XVw>.

B. Relation to Causal-Inference

From a formal causal inference perspective (Pearl, 2000), our event tree is the part of our approach that reflects the formal “Structured” Causal Model (SCM), because it is a generative model that reflects the data generation process, and it can account for complex dependencies between events. The DAG representation (Section 4.2) is useful for

reasoning about semantic instructions, but we intentionally avoid from naming it a *Causal* DAG, because it can't represent dependencies between events that are not explicitly observed in the video. E.g., in the example $[(A, B), (C, D), (A, E)]$ in Section 4.2, it may be that (A, E) depends on (C, D) because C blocks D from reaching to E before A do. The event tree can simulate this behaviour, while the DAG $(C, D); (A, B) \rightarrow (A, E)$ is unaware of it.

C. Additional experimental details

C.1. Random Baseline

We sample an intervention at random from an estimated distribution of ground-truth interventions. The distribution is estimated by calculating a 2D-histogram with 30×30 , and approximating the distribution within each bin to be uniform.

C.2. Sequential Baseline

We used the validation set to select the number of layers for this baseline, $\in [5, 10, 20, 30]$. There wasn't any significant difference when using 5 or 10 layers, and the success rate degraded for 20 or 30 layers. Therefore, we used 5 layers for evaluating performance on the test set.

C.3. Instruction ablation Baselines

We report the "count" and "ancestor" ablations by zeroing their respective features in the instruction and using the same model weights that were used to report the performance of the ROSETTE model. We did not retrain the model for these cases because the ROSETTE model was trained to handle these cases, as is evident by the "Unconstrained" metric.

For ablating the "full" instruction, we retrained the model, while completely zeroing the representation vector of the input instruction.

D. Data generation details

D.1. Video generation details

In this section, we describe the generation process of the dynamical scene. We first create an "unperturbed" video. Then, we perturb the video by modifying the velocity of a specific element, which will be later designated as the pivot. We let the perturbed video roll out, validate that it is indeed semantically different than the unperturbed video, and label it as the "observed" video. The unperturbed video can now be used as reference for our instruction generation process. It is a realization of a specific, complex, semantic chain of events that is both semantically different than the perturbed ("observed") video and is also feasible, e.g, by setting the intervention value as to revert the perturbation. This flow

guarantees that we can ask meaningful instructions on the "observed" that are guaranteed to be realizable.

The unperturbed video. We construct the unperturbed video by iteratively adding spheres and collisions in a physical simulator (IsaacGym (Makoviychuk et al., 2021)) increasing the video complexity. We start by placing a sphere in the confined four-walled space and assign it a random velocity.

The dynamics of a sphere moving freely in a confined square area can be expressed analytically. We pick a random time t_1 , hitting velocity, and hitting angle for the first collision. We analytically solve for the initial position and velocity at $t_0 = 0$ that will result in the a collision at t_1 with the specific hitting velocity and angle. We assign these value to a randomly colored sphere.

Due to discrepancies between the simulator dynamics and the kinematic analytic model, we roll out the dynamical system in the simulator, and record the system configuration immediately after a collision.

We continue adding spheres iteratively. Given a dynamical configuration at t_i , we randomly select a sphere O_i from the existing spheres, collision time t_{i+1} , hitting angle and velocity. We solve analytically and find the initial position and velocity at $t_0 = 0$ that will result in a collision with O_i corresponding parameters. We roll out the dynamical system, and update the velocities and positions records after each collision with the empirical values from the simulator.

Our simple kinematic model assumes the target sphere and the newly added move freely. However, other spheres may cross their trajectories, resulting in an a collision that will distract the spheres from their designated path. However, this simply means that the planned random collision was replaced by a different collision. Since we update our records of the resulting collisions and corresponding output velocities and positions using the simulator, this does not pose any serious limitations.

The observed video. We pick a random sphere from the set of spheres and assign it a different velocity at $t = 0$. We roll out the system in the simulator and log all resulting collisions. We validate that the resulting collision sequence is different than the unperturbed video collision sequence. We now have two videos that differ only in the initial velocity of a specific sphere, but result in a substantially different semantic chain of events.

D.2. Instruction generation details

We describe the instruction generation process when given an "observed" video, and a "counterfactual" video that displays an alternative cascade of events.

Given a ground-truth video, its sequence of collisions, and

a pivot, we randomly sample an instruction: Starting by randomly sampling a target collision from the sequence. And then, we randomly sample up to two constraints that accompany the goal. For constructing the constraints, we first represent the sequence of collisions using a DAG, in a similar fashion as described in Figure 3, then we use standard NetworkX functionality (Hagberg et al., 2008) for graph traversal: (1) We use “dag.ancestors()” to get a list of nodes for the “ancestor” constraint. (2) We use “all_simple_paths()” to count the nodes in a chain reaction between the pivot and the target collision.

To avoid trivial goals, we drop an instruction if it is fulfilled by the observed video (rather than the “counterfactual” video). We sample up to 5 unique instructions for each scene (~4 on average).

D.3. Instruction feature representation

We assume perfect lexical perception, and provide the agent with the a structured vector representation of each instruction, by concatenating the following fields [**target_obj_a**, **target_obj_b**, **pivot_obj**, **ancestor_obj_a**, **ancestor_obj_b**, **ancestor_ind**, **count**, **count_ind**]: Where **target_obj_a**, **target_obj_b** are the object representations of the target collision. **pivot_obj** represents the pivot. **ancestor_obj_a**, **ancestor_obj_b**, **ancestor_ind** represent the two “ancestor” objects and a binary indicator scalar. If an “ancestor” constraint is not applicable for an instruction, we them all to 0. **count**, **count_ind** are 2 scalar values: One for the number of collisions of the chain “count” constraint, and another used as a binary indicator for the “count” constraint. Similarly if a “count” constraint is not applicable for an instruction, we both **count** and **count_ind** to 0.

Finally, note that each object is represented by a one-hot vector $\in \mathbb{R}^{12}$, because the environment has 12 types of unique objects: 6 colored balls, 2 static pins, and 4 walls.

D.4. Complex instructions dataset

For the complex instructions dataset, we add a third object centric constraint that counts the number of interactions a specific object makes on the paths from the pivot to the target collision. It resembles constraining the amount of resources available per instance on a logistic chain. With an additional constraint we can test our approach on a more challenging task that has a large variety of instructions that have 2 or more constraints. We split the evaluation set to “Hard” instructions that have 2 or more constraints, and “Easy” instruction with 0-1 constraints. We generated instructions for the same scenes as in the main dataset, which yields ~4.5 instructions per scene. The test set consists of 2190 episodes, where 54% are “Hard” instructions.

E. Implementation details of the model of the Value function

We use a Graph Neural Network (GNN) to parameterize our value function. We represent the graph as a tuple (A, X, E, z) where $A \in \{0, 1\}^{n \times n}$ is the graph adjacency matrix, $X \in \mathbb{R}^{n \times d}$ is a node feature matrix, $E \in \mathbb{R}^{m \times d'}$ is an edge feature matrix, and $z \in \mathbb{R}^{d''}$ is a global graph feature. we chose to use a popular message passing GNN model (Battaglia et al., 2018) that maintains learnable node, edge and global graph representations.

Architecture The model is composed of several message passing layers, $L^k \circ \dots \circ L^1$ where each L^i updates all representations, i.e.:

$$X^{i+1}, E^{i+1}, z^{i+1} = L^i(A, X^i, E^i, z^i; \theta^i),$$

Each layer L_i updates the features sequentially: the node and edge features are updated by aggregating local information, while the global feature is updated by aggregating over the whole graph. We denote the parameters of the MLPs that are used in a layer L_i as θ_i , and note that these are the only learnable parameters in the model. At the last layer $i = k$ we use a single dimension for the global feature, i.e., $d' = 1$, which is then used as the value of the event node.

Feature representation We describe next the feature representation of the inputs to the node feature matrix X , the edge feature matrix E , and the global graph feature z .

We start by describing a feature representation of any of the dynamic and static objects in the scene: An object o is represented by concatenating the following fields **obj_feat**(o) = [**one_hot**(o), **is_stationary**, **is_active**, **instruct_inner_prod**, **ancestor_ind**, **count**, **count_ind**]: Where **one_hot**(o) is a one-hot vector $\in \mathbb{R}^{12}$, as represented by the instruction; **is_stationary** indicates whether the object is stationary; **is_active** means that in the context of a current collision, the object dynamics were coming from a collision chain that included the pivot; **instruct_inner_prod** is the results of an inner product of **one_hot**(o) with each of the 5 object representations at the instruction embedding (Section D.3). Finally, **ancestor_ind**, **count**, **count_ind** are copied from the instruction embedding.

The graph node and edge features are derived from the DAG representation (Figure 3). Each row of the node feature matrix X concatenates the two objects that participate at a collision [**obj_feat**(obj_a), **obj_feat**(obj_b)]. Each row at the edge feature matrix E represents **obj_feat**(o) of the object on that edge.

Last, the global feature z is a copy of the instruction embedding described in Section D.3.

F. The forward model

The forward module takes as input a world state w_i it outputs the next semantic event (s'), and dynamic configuration $f(w_i) = w'_i = (c'^1_i, c'^2_i, \dots, c'^n_i, t'_i)$ immediately after the predicted semantic event at t'_i . The section is divided into three parts. First, we describe the analytical equations that control if two objects will collide. Then we show how can leverage the analytic model to efficiently branch out from a node in the event tree. Finally, we fill in the missing details and present the full forward model.

The collision detector. Assume two spheres $i = \alpha, \beta$ moving freely on a plane with an initial velocity of \mathbf{v}_i and position \mathbf{p}_i at $t = 0$. Each sphere has a radius of r_i . If the two spheres collide, then, at the moment of collision, the spheres intersect at a single point. A simple geometric calculation shows their planar distance at collision is

$$d = 2\sqrt{\|\mathbf{r}_\alpha\| \|\mathbf{r}_\beta\|}.$$

Therefore, in order to check if the spheres collide, we can check if the distance between the two spheres is ever equal to d ,

$$\|\mathbf{r}(t)\|^2 = \|\mathbf{r}_\alpha + \mathbf{v}_\alpha \cdot t - \mathbf{r}_\beta - \mathbf{v}_\beta \cdot t\|^2 = d^2$$

This is a quadratic equation in t , which we can solve for analytically. If the discriminant is non-negative, the collision time corresponds to the smaller root. The spheres' velocities immediately after the collision are given by:

$$\begin{aligned} \mathbf{v}'_1 &= \mathbf{v}_1 - \frac{2m_2}{m_1 + m_2} \frac{\langle \mathbf{v}_1 - \mathbf{v}_2, \mathbf{x}_1 - \mathbf{x}_2 \rangle}{\|\mathbf{x}_1 - \mathbf{x}_2\|^2} \cdot (\mathbf{x}_1 - \mathbf{x}_2) \\ \mathbf{v}'_2 &= \mathbf{v}_2 - \frac{2m_1}{m_1 + m_2} \frac{\langle \mathbf{v}_1 - \mathbf{v}_2, \mathbf{x}_1 - \mathbf{x}_2 \rangle}{\|\mathbf{x}_1 - \mathbf{x}_2\|^2} \cdot (\mathbf{x}_2 - \mathbf{x}_1) \end{aligned}$$

Likewise, it is trivial to obtain an analytical expression for the collision time and output velocity of a collision between a freely moving sphere and each of the static walls bounding the spheres (should the collision occur).

Parallelizing collision detection. The collision detector provides an analytic condition that validates whether a specific collision occurs. Therefore, we can solve it in parallel for multiple tuples of $(\mathbf{r}_1, \mathbf{v}_1, \mathbf{r}_2, \mathbf{v}_2)$ on a GPU using packages such as PyTorch. Therefore, given an intervention set of X_u , and a corresponding world-state set W_u , we iterate over all possible collisions $S_{ij} = (O_i, O_j)$ and apply our collision detector on all $w \in W_u$ simultaneously. The complexity is quadratic in the number of object rather than linear in the number of interventions. This allows us to apply our algorithm with a high number of interventions,

and therefore enable us to consider delicate sequences of collision that would require refined "trick shots".

This approach considers every two objects O_i, O_j as moving freely. However, another object in the environment, e.g. O_k , may interact with O_i (without loss of generality) before the collision. This necessarily means that the collision time t_{ik} precedes t_{ij} . In order to account for this, we hold an additional structure that maintains the minimal collision time for every $w \in W_u$. We update it as we iterate over all possible collisions. Then, we associate each $w \in W_u$ and its corresponding $x \in X_u$ to the event node corresponding to the collision with the earliest collision time.